Journal of Polymers and the Environment
https://doi.org/10.1007/s10924-020-02019-9

ORIGINAL PAPER

Effect of Sugar Palm Fiber (SPF) to the Structural and Optical Properties of Bioplastics (SPF/Starch/Chitosan/Polypropylene) in supporting Mechanical Properties and Degradation Performance

Oktavianus Sardy Jangong[1] · Heryanto Heryanto[1] · Roni Rahmat[1] · Inayatul Mutmainna[1] · Paulus Lobo Gareso[1] · Dahlang Tahir[1]

Accepted: 15 December 2020
© The Author(s), under exclusive licence to Springer Science+Business Media, LLC part of Springer Nature 2021

Abstract

Recycling plastic waste by mix with natural polymers for bio-plastic packaging produces plastics with high mechanical properties and easily degradable. In this study, the relation between the structural and the optical properties of composite SPF/starch/chitosan/polypropylene to the mechanical properties and degradation performance were analyzed. Structural and optical properties of composite bioplastic SPF/Starch/Chitosan/Polypropylene have analyzed using X-Ray diffraction (XRD), and Fourier transforms infrared (FTIR) spectroscopy, respectively. The composition was varied: the ratio between starch and chitosan are 35/65, 50/50, and 65/35 with additional SPF for each ratio is 1%, 3%, and 5%. The SPF effectively enhances the tensile strength due to the SPF's better dispersion and interaction in the starch/chitosan/polypropylene matrix. For SPF's effect on the degradation performance, the ratio starch/chitosan 50/50 increase for 1% SPF is 87.23%, for 3% SPF is 92.59%, and for 5 SPF is 94.12%. The refractive index (n), extinction coefficient (k), dielectric functions (ε), and energy loss function (Im $(-1/\varepsilon)$) determined from the quantitative analysis of FTIR spectra by using Kramers–Kronig (K–K) relations. The crystalline phase increases with increasing the amount of SPF in composite bioplastic SPF/Starch/Chitosan /Polypropylene for ratio starch/chitosan is 35/65, which consistent with the distance between the wavenumber (D) of transversal and longitudinal optical phonon vibration mode become wider. We found that a good correlation between optical properties, structural properties, mechanical properties, and degradation performance for ratio starch/chitosan 35/65 and 50/50 with SPF 1% and 3% in the composite. Besides, the FTIR spectra could be useful for determining the optical phonon vibration, dielectric function, and energy loss function of composite bioplastic SPF/Starch/Chitosan /Polypropylene. The degradation performance by additional polypropylene from plastic waste shows a potential solution for decreasing plastic waste in the world.

Keywords Sugar palm fiber (SPF) · Polypropylene · Tensile strength · Optical properties · Crystalline phase · FTIR

Introduction

Packaging from plastic synthetic widely used in daily life for: food industry, biomedical fields, electronic, and agriculture packaging, but it harms the environment [1]. The process of recycling or disposing of plastic waste by minimizing the side effects of residual waste on humans and environments is one of the main challenges today. Polypropylene (PP) is the most dominant packaging material due to the excellent processing performance and versatility with a melting point of 160 °C [1, 2] Polypropylene high hydrophobic, water repellence, and high molecular weight with the main contents are carbon and hydrogen, which are similar structures with polyolefin and polyethylene [3]. Although it has high mechanical strength, these materials cannot be degraded in a short time naturally. Therefore, recycling plastic waste to be useful and easily degradable is necessary to mix with natural polymers for bio-plastic packaging. [2].

Natural polymers are low mechanical properties, cannot stand at high temperatures, and brittle but easily decomposed by microorganisms. Therefore, the mixing of synthetic plastics with natural fibers is expecting to produce plastics

✉ Dahlang Tahir
dtahir@fmipa.unhas.ac.id

[1] Department of Physics, Hasanuddin University, Makassar 90245, Indonesia

Published online: 01 January 2021

Content courtesy of Springer Nature, terms of use apply. Rights reserved.

that have high mechanical properties [1, 3]. Bioplastics from starch and chitosan are renewable natural polymers that pass through the thermo-mechanical process in suitable plasticizer mixtures such as glycerol. Starch is a glucose polymer, which is composed of two types of polysaccharides, namely amylose and amylopectin. This is an important ingredient for producing biofilms or bioplastics for the food and pharmaceutical industries. However, starch films are too fragile and need plasticization. The plasticizer affects the optical properties, structural properties, mechanical properties, and water vapor permeability [4]. Wood or cellulose potential to be used to increase the mechanical properties of composite. However, for industrial-scale leading to over-exploitation of forests, it negatively affects the climate and the environment. On the other hand, the destruction of these materials by burning or spoilage is a pollutant. A viable alternative is regenerative use materials obtained from plants or other plants with low pollution potential. Starch is one of the most promising material for this purpose because it can be easily obtained from corn, potatoes, or vegetables fully recyclable without toxic residues [5, 6].

The previous studies reported that using starch and chitosan reinforced polypropylene for high mechanical properties of bio-plastic [7, 8]. Reinforcing fillers such as cellulose from natural fibers is an alternative solution to improve mechanical properties. Sugar palm fibers (SPF) are obtained from the trunk of the tree, which is winding from the top down. All across the countries, natural fiber has become famous as an important ingredient in many industries applications. This opportunity has paid a lot of attention to scientists to learn more about SPF as a reinforcement in polymer composites [9, 10]. The color of SPFis brown to black, the diameters ranging between 99 µm and 311 µm, and the density about 1.05 g/cm^3 which the tensile properties are increased depends on the size of the fiber due to the cellulose content [11]. As the researches development, palm fiber is proven to have many significant advantages to be considered; environmentally friendly, low price, and abundant in nature. While in terms of properties, palm fiber has low density, good mechanical properties, and good thermal properties [12].

Recently fiber from natural resources has been used for bio-plastic applications from oil palm empty fruit bunch, water hyacinth, cotton and sugarcane bagasse, and many other sources [13–17]. Several experiment techniques, plasticizers, and properties were reporting for producing the bioplastic composites starch-based [18–21].

The various concentration of SPF and ratio of starch/chitosan in the form of composite SPF/starch/chitosan/polypropylene affected the structural, mechanical, magnetic, optical, and degradation properties [7, 8, 22]. The relation between the structural properties and the optical phonon vibration for composite SPF/starch/chitosan/polypropylene to the mechanical properties and degradation performance has not been experimentally investigated adequately. These properties are fundamental knowledge to understand the mechanism and the relation between these properties to the processes of biodegradation performance. Hence, in this study, we focus on the quantitative analysis of the X-Ray diffraction (XRD) spectra for determining the structural properties (the percentage of amorphous and crystalline phase) and the Fourier transform infrared (FTIR) for determining the refractive index (n), extinction coefficient (k), and dielectric function (ε), and energy loss function (Im $(-1/\varepsilon)$). From these analyses, we continue to find the optical phonon vibration in the form of longitudinal (LO) and transversal (TO). We also find the relation between these types of optical vibration and the structural properties to the mechanical properties and biodegradation performance for the various amount of SPF in composite SPF/starch/chitosan/polypropylene to understand the effect of each other's properties on the performance of these materials.

Experiment

Material

Sugar palm fibers (SPF) were taken from Makassar, South Sulawesi, Indonesia. Polypropylene composite synthesized from cup plastic waste, aquades, sago starch, chitosan (deacetylation rate of 94.88%; molecular weight, 200 Kda–500 Kda; 200–300 mesh particle size; viscosity 55.31 mPa), Glycerin (Merck), Acetic Acid (CH_3COOH) (6%) (Merck), NaOH (5%).

Bioplastics Synthesis

SPF immerse in NaOH 5% solution for 1 h to remove dirt and surface hemicellulose at the fiber's surface. The SPF cleaned using distilled water and then dried at temperature 125 °C for 10 min [23], filtered using a ten mesh, and SPF ready for further use.

Polypropylene (plastics waste) was dissolved into glycerin and heated by hot magnetic stirrer at temperature of 350 °C for 2 h. Then, sago starch was a mixture with aquades by magnetic stirrer at temperature 100 °C. Acetic acid (CH_3COOH) poured into chitosan and stirred until formed gel. The various ratio between starch and chitosan are 35/65, 50/50, and 65/35, with additional SPF for each composition; 1%, 3%, and 5%. Then, a polypropylene solution poured into the glass beaker containing SPF/starch/chitosan solutions. Subsequently, all solution materials were mixed and stirred at temperature 100 °C for 20 min with 600 rpm until homogenized and formed bio-plastic solution. After that, the bioplastic solution poured into a sample container and dried at

Content courtesy of Springer Nature, terms of use apply. Rights reserved.

85 °C for 16 h. The bioplastics synthesis process can be seen in Fig. 1, and the corresponding mass for each component of the biofilms are presented in Table 1.

Characterization of Bioplastic

The amount of crystalline and amorphous phase of bio-plastic composite SPF/starch/chitosan/ polypropylene analyzed by using powder X-Ray diffraction (XRD) Shimadzu 7000 with CuKα radiation sources (λ = 1.5405 Å) in the range diffraction angle 2Θ from 15 to 60°, operates at 30 kV and 10 mA. FTIR spectrometer (Shimadzu Corp.) IRPrestige-21 use for determining functional groups in bio-plastic composites SPF/starch/chitosan/ polypropylene at the wavelength 3800–800 cm^{-1}. The mechanical properties are determining by using a texture analyzer (Texture Analyser AND MCT-2150). The size of bioplastic films is 2 × 5 cm for texture analyzer with crosshead speed setting is1 mm/min and crosshead return speed is10 mm/min. Biodegradability tests are performing by measure the rate of weight loss (W_{loss}) of bioplastic films after the sample burying in the soil for a specific time calculated by $W_{loss} = (W_i - W_f)/W_i$ where W_i is initial weight and W_f is weight after biodegradability [24]. Bioplastic films with a size of 2 × 1cm are weighted (W_i) and then hiding in the ground for 5 cm below the soil's surface. After 3 days, 7 days, 14 days, and 28 days, samples are dug out of the soil, washed with distilled water, then the sample was reheated in the oven at 85 ºC for 10 min and weighed (W_f) [24].

Table 1 Corresponding mass from the Fig. 1 for each component of composite bioplastic SPF/starch/chitosan /polypropylene: starch, chitosan, polypropylene (PP), and additional sugar palm fiber (SPF): 1% (0.052 gr), 3% (0.156 gr), and 5% (0.260 gr) for each R(S/C) (Ratio: (Starch/Chitosan))

R(S/C) (%)	Starch (gr)	Chitosan (gr)	PP (gr)	Total (gr)
35/65	2.08	1.12	2	5.2
50/50	1.60	1.60	2	5.2
65/35	1.12	2.08	2	5.2

Data Analysis

The crystalline phase X_c obtained from XRD spectra by the empirical method [25] where I_{am} and I_{002} are the area of

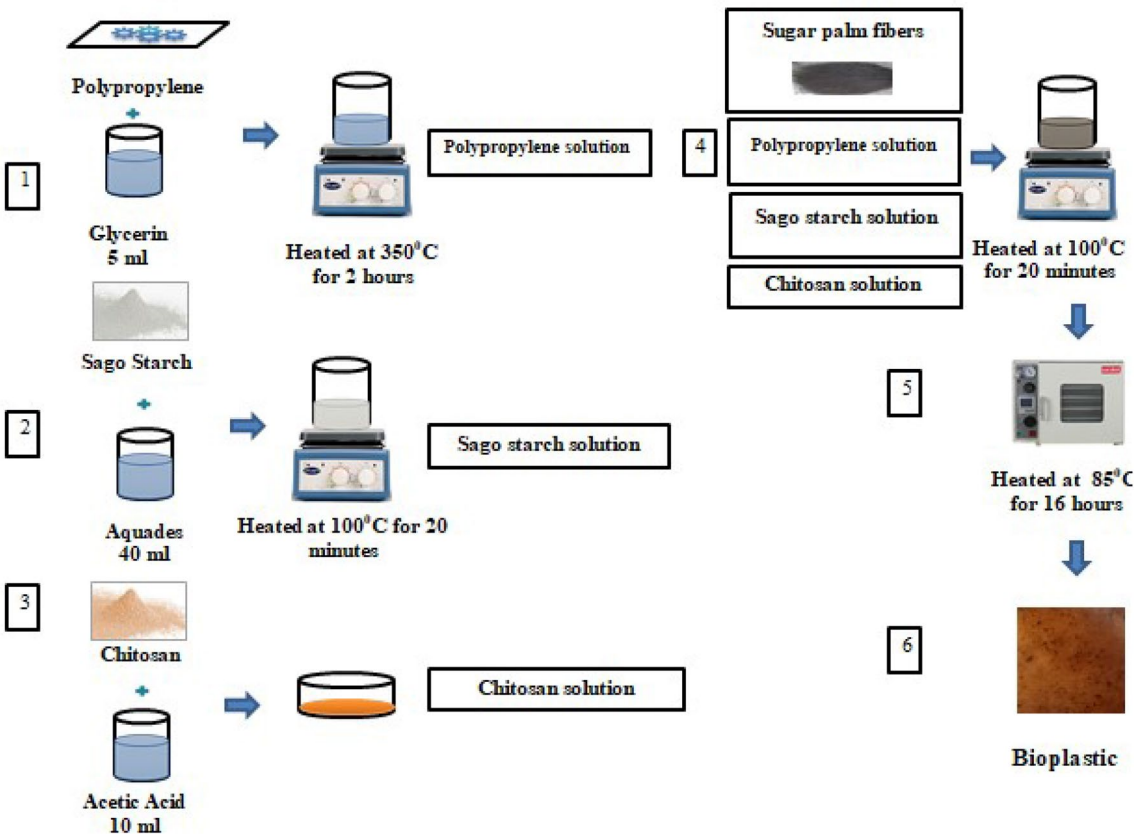

Fig. 1 Illustration of synthesizing processes for bio-plastics composite SPF/starch/chitosan/polypropylene with different ratio of starch/chitosan and various amount of SPF in this study

Content courtesy of Springer Nature, terms of use apply. Rights reserved.

amorphous and crystalline phase (002), respectively, determined by the following equation:

$$X_c = \frac{I_{002} - I_{am}}{I_{am}} \times 100\% \quad (1)$$

The optical properties, dielectric function, and energy loss function determined from the quantitative analysis of FTIR spectra. The transmittance spectra from the FTIR spectra is need to be converted to the reflectance spectra by the following equation [26]:

$$A(\omega) = 2 - \log[T(\omega)\%] \quad (2)$$

$$R(\omega) = 100 - [T(\omega) + A(w)] \quad (3)$$

The reflection spectra is used for determining the real part of refractive index $n(\omega)$ and imaginary part of refractive index $k(\omega)$ as follows [27, 28]:

$$n(\omega) = \frac{1 - R(\omega)}{1 + R(\omega) - 2\sqrt{R(\omega)}\cos\varphi(\omega)} \quad (4)$$

$$k(\omega) = \frac{2\sqrt{R(\omega)}sin\varphi(\omega)}{1 + R(\omega) - 2\sqrt{R(\omega)}\cos\varphi(\omega)} \quad (5)$$

where $\varphi(\omega)$ is the phase change between the reflection and the incident photon signals in the FTIR spectroscopy:

$$\varphi(\omega) = -\frac{\omega}{\pi}\int_0^{\infty} \frac{\ln R\left(w'\right) - \ln R(\omega)}{\omega'^2 - \omega^2} \quad (6)$$

By applying K-K relation, the equation (6) become:

$$\varphi\left(\omega_j\right) = -\frac{4\omega_j}{\pi} x\Delta\omega x \sum_i \frac{\ln(\sqrt{R(\omega)})}{\omega_i^2 - \omega_j^2} \quad (7)$$

j is a series of wavenumber, if j is an odd number so then i parts is 2,4,6,8,...,j−1,j+1 and while wavenumber j is an even, i parts is 1,3,5,7,...,j−1,j+1,... $\Delta\omega = \omega_{i+1} - \omega_i$.

The $n(\omega)$ and $k(\omega)$ are the input parameter in determining the real part $\varepsilon_1(\omega)$ and the imaginary part $\varepsilon_2(\omega)$ of the dielectric function from the relations:

$$\varepsilon_1(\omega) = n^2(\omega) - k^2(\omega) \quad (8)$$

$$\varepsilon_2(\omega) = 2n(\omega)k(\omega) \quad (9)$$

Degradation performance is determining in the form of the weight loss *Is* (%) of bio-plastic as follows [29]:

$$I_s = \frac{W_o - W}{W_o} \text{ x } 100\% \quad (10)$$

where W_0 is the weight before placement on the ground and W is the weight after a certain time on the ground.

Results and Discussion

XRD Analysis

The XRD pattern of bio-plastics are shown in Fig. 2a for various ratio starch/chitosan and SPF (a) 1%, (b) 3%, and (c) 5%. The crystalline phase increase with increasing the amount of SPF for the same ratio starch/chitosan (R(S/C)) in the composite, ex. for R(S/C) is 35/65 shows an increase from 7.89% for 1% SPF to 15.58% for 5% SPF as shown in Table 2. For the ratio R(S/C) is 50/50 with 5% SPF, the crystalline phase decreases sharply may due to starch and chitosan covering the SPF properly, consequently hindering the crystalline phase [30–35] that increase the amorphous phase. The intensity of diffraction peak influence to the crystalline phase indicated well-ordered structure due to the silica-containing fibers in the composite was removed [19, 36, 37]. Starch and chitosan have the hydrophilic, water molecules can be absorbed by the sample, and transferred to the interlayer domain for a period of moisture equilibrium [38].

FTIR Analysis

Figure 2b shows FTIR spectra of composite bio-plastic SPF/starch/chitosan/polypropylene for various SPF and the ratio starch/chitosan. There are four main absorption peaks: the bonding vibration of the O–H stretching, C–H stretching, C=C stretching and C–O stretching [7, 39]. O–H bonding at 3381 cm^{-1} which indicated polysaccharides and alcohol. C–O stretching at 1037 cm^{-1} of ribbon is along with the addition of the starch and SPF containing lignin and cellulose. All peaks are found in the same range indicated that the SPF is not significantly affected the bonding configuration in composite [40]. The absorbance band located at 3100–3700 cm^{-1} identified as O–H vibration.

The cellulose can be identified through the absorptions peak at 2933 cm^{-1} (C–H alkane vibrations), and 1037 cm^{-1} (stretching C–O ester) [7, 8]. For the absorbance at 1643 cm^{-1} is stretching aromatic ring of C=C from the SPF in the lignin or starch [41]. However, these peaks were decrease when the ratio starch/chitosan is increasing in the composite probably due to the starch covering and bonding the SPF properly, consequently hinder the lignin and hemicellulose. Besides that, the absorbance peak 1000–1300 cm^{-1} indicated the presence combination of C–O and C–H stretching groups [31, 42].

The optical properties, dielectric function, and energy loss function as a function of wavenumber determined from the quantitative analysis of FTIR spectra by applying K-K

Content courtesy of Springer Nature, terms of use apply. Rights reserved.

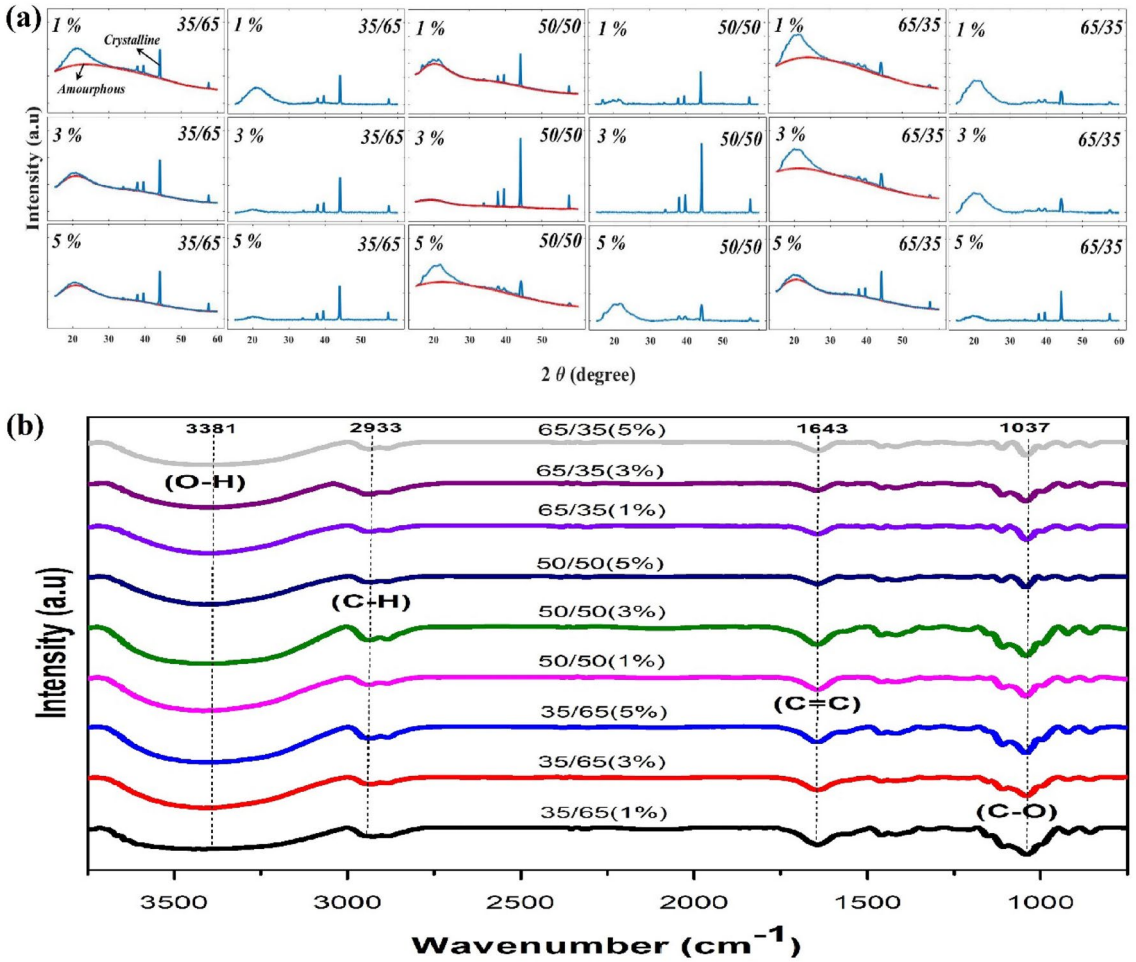

Fig. 2 X-Ray diffraction (XRD) spectra (**a**) and Fourier transform infrared (FTIR) spectroscopy spectra (**b**) of composite bio-plastic SPF/starch/chitosan/ polypropylene for different ratio starch/chitosan and various amount of SPF (1%, 3%, and 5%)

Table 2 Optical phonon vibration mode for transversal (TO), longitudinal (LO), and the difference between LO and TO (Δ) determined from quantitative analysis of FTIR spectra in Fig. 3

SPF		1%			3%			5%	
R(S/C)	35/65	50/50	65/35	35/65	50/50	65/35	35/65	50/50	65/35
TO (cm^{-1})	1024	1026	1024	1026	1018	1028	1036	1031	1026
LO (cm^{-1})	1178	1188	1091	1263	1278	1280	1274	1082	1170
Δ (cm^{-1})	154	162	67	237	260	252	238	51	144
A (P) %	92.01	83.60	91.71	92.07	73.70	84.20	84.41	91.34	85.51
C (P) %	7.98	16.39	8.28	7.98	26.29	15.79	15.58	8.65	16.48
TS (MPa)	25.02	27.42	40.01	55.23	57.06	59.02	63.24	63.35	78.00
D 21 (%)	82.58	70.21	67.89	88.24	59.26	64.29	71.88	82.85	54.05
D 28 (%)	90.43	87.23	86.24	98.04	92.59	80.95	90.63	94.12	77.03

Amorphous phase (A(P)) and crystalline phase (C(P)) determined from the XRD spectra in Fig. 2b. Tensile strength (TS), degradation for 21 days (D 21), and degradation for 28 days (D 28) of composite bio-plastic SPF/starch/chitosan/polypropylene for different ratio starch/chitosan (R(S/C)) and various amount of sugar palm fiber (SPF) 1%, 3%, and 5%

relation [43–46]. The K-K relation also usually used in quantitative analysis of electron spectroscopy spectra as a function of energy loss [47–55]. The quantitative analysis's optical properties are in the form refractive index $n(\omega)$ and extinction coefficient $k(\omega)$, complex dielectric function, and the energy loss function.

Content courtesy of Springer Nature, terms of use apply. Rights reserved.

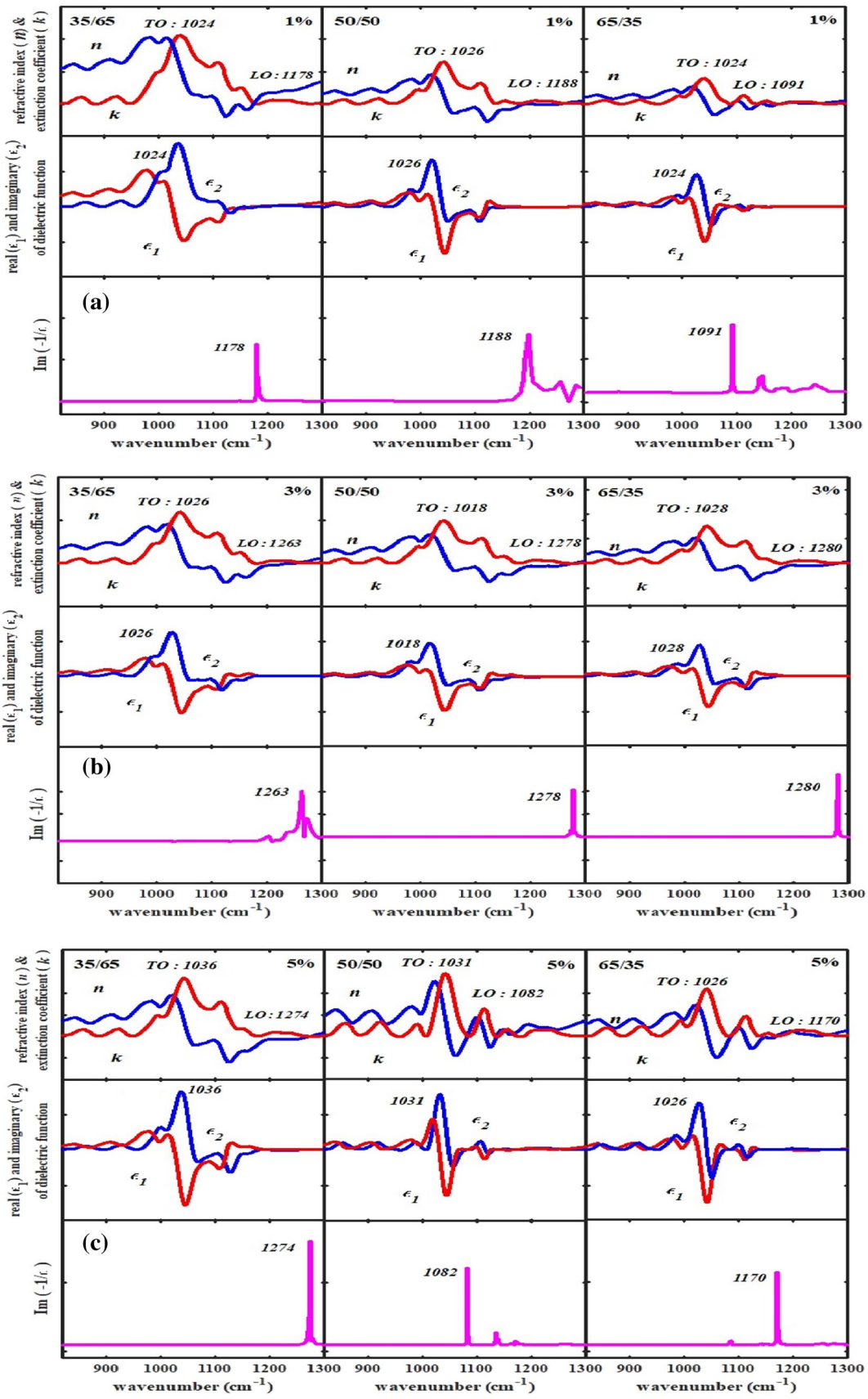

Content courtesy of Springer Nature, terms of use apply. Rights reserved.

◂**Fig. 3** Quantitative analysis of FTIR spectra in determining optical properties (first rows), dielectric function (second rows), and energy loss function (third rows) of composite bio-plastic SPF/starch/chitosan/polypropylene for various ratio starch/chitosan with 1% SPF (**a**), 3% SPF (**b**), and 5% SPF (**c**)

The optical properties is presented in the top row of Fig. 3a for 1% SPF, Fig. 3b for 3% SPF, and Fig. 3c for 5% SPF. The cross point between n and k is related to the optical intersection with the lattice indicated by TO at a lower wavelength for transverse optical and LO at a higher wavelength for longitudinal optical phonon vibration mode for more detail see Table 2. The difference between LO and TO (Δ = (LO−TO)) is increases with increasing the ratio between starch and chitosan (R(S/C)) as can be seen for 1% SPF and 3% SPF but not for 5% SPF may due to the cross-linking is not bonding properly between SPF and starch/chitosan.

Dielectric Function

Figure 3 shows the results of quantitative analysis of FTIR spectra for 1% SPF (a), 3% SPF (b), and 5% SPF (c). The first rows of Fig. 3a–c shows the refractive index (n) and extinction coefficient (k), second rows is the real ($\varepsilon_1(\omega)$) and imaginary parts ($\varepsilon_2(\omega)$) of the dielectric function, and the third rows is the energy loss function (Im $(-1/\varepsilon\ (\omega))$. The main peak of $\varepsilon_2(\omega)$ also used to identified of the TO phonon vibration mode. The high confidence analysis result for TO phonon vibration mode wavenumber position if the wavenumber position between the cross point of n and k (first rows) consistence with the main peak of $\varepsilon_2(\omega)$ (second rows). For the ratio starch/chitosan is 35/65, the main peak position of $\varepsilon_2(\omega)$ shifted to the higher wavenumber position with increasing the SPF from 1 to 5% in the composite may due to the cross-linking bonding rearranged to form a new structure [43, 56]. Another ratio that shows fluctuation may due to the effect of cohesion forces between the SPF and the plasticizer from polypropylene. It's phenomena caused by the non-uniformity cross-linking and less stable structure in the composite.

For LO vibration modes, firstly identified from the intersection between $n(\omega)$ and $k(\omega)$ (first rows) of Fig. 3a–c and the second, by the main peak of energy loss function (Im $(-1/\varepsilon\ (\omega)) = (\varepsilon_1(\omega))\ /\ ((\varepsilon_1^2(\omega)+\varepsilon_2^2(\omega))$ (third rows) of Fig. 3a–c [43]. The best results indicated by the same wavenumber positions for these two methods. Energy loss function usually determined from the quantitative analysis of electron spectroscopy spectra [57–59] and the main peak position consider as the plasma frequency. Similar to the quantitative analysis from the FTIR spectra for composite cement/$BaSO_4$/Fe_3O_4, for geopolymer fly ash-metal [60] and composites Fe/CNs/PVA [61] shows that the main peak position of (Im $(-1/\varepsilon\ (\omega))$ is the plasma frequency [43].

Tensile Strength

To clarify the effect of SPF to the tensile strength, we determined the tensile strength of composite bio-plastic SPF/starch/chitosan/polypropylene for various SPF and the different ratio of the starch/chitosan. Figure 4 shows the tensile strength increases significantly with the increase in the SPF amount in the composite. Indicated that the SPF could effectively enhance the tensile strength of the composite bioplastic SPF/starch/chitosan/polypropylene. The probability that the SPF has better dispersion and interaction in the starch/chitosan/polypropylene matrix. The strength of SPF come from the cellulose, as reported for Ibrahim, Sapuan, Zainudin, Zuhri [62] due to the some of the lignin and hemisellulose of SPF remove after immersed in the NaOH [40].

The tensile strength is increase with increasing the ratios of the starch/chitosan (R(S/C)), for 1% SPF increases from 25.02 to 40.01 MPa, for 2% SPF increases from 55.23 to 59.02 MPa, and for 5% SPF increases from 63.24 to 78.00 MPa, respectively from lower R(S/C) to higher R(S/C). It shows that the tensile strength increase with increasing the amount of SPF in the composites bioplastic. The lowest range tensile strength is for 1% SPF and the highest is for 5% SPF as shown in Fig. 4 and corresponding data is presented in Table 2. The tensile strength increases with increasing the starch/chitosan ratios due to the interface formation of hydrogen bonding from the NH^{3+} cation from chitosan with OH^- backbones-anions from the starch [63].

Biodegradation Test

Biodegradation of composite bio-plastic SPF/starch/chitosan/polypropylene in this study for various amount of SPF (1%, 3%, and 5%) as shown in Fig. 5. The degradation for all composition at 28 days grounded is > 80% which is in the soil may the microorganisms and moisture play an important role for degradation process [7, 8]. Water also can accelerate biodegradation by absorption processes of the bio-plastic causes swelling [64]. For the starch content in bio-plastic up to 50% of their weight, then they can easily absorb water, consequently will be very rapid biodegradation [65, 66]. For the effect of SPF can be seen for 28 days in Table 2 shows for ratio starch/chitosan 50/50 increase for 1% SPF is 87.23%, for 3% SPF is 92.59%, and for 5% SPF is 94.12%. For ratio starch/chitosan is 65/35 shows decreases degradation with increasing the amount of SPF may due to the crystalline phase (ordered structure) increase, which affected to the ability in absorbing water [63].

Figure 6 shows the illustration of the degradation process naturally. The step processes of biodegradation are divided by; first, catalyzed biologically, in this phase, enzymes and decomposition chemicals act as catalysts for plastic biofilm. During this time, aerobic microbes are

Content courtesy of Springer Nature, terms of use apply. Rights reserved.

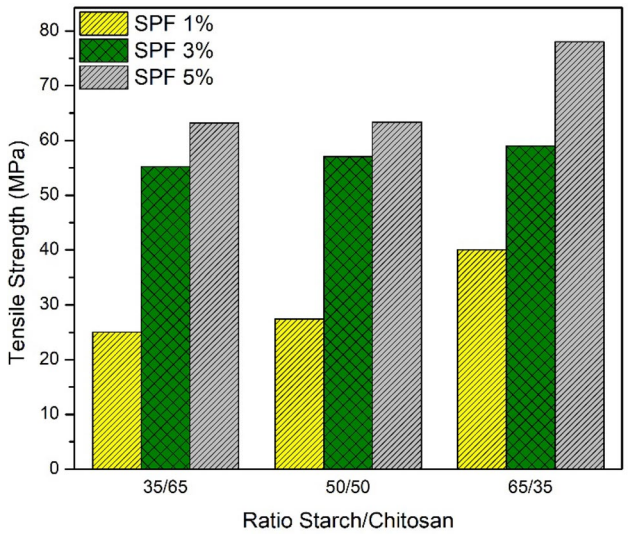

Fig. 4 Tensile Strength for bioplastics composite SPF/starch/chitosan/polypropylene with different ratios of starch/chitosan and various amount of SPF in this study

formed, and water vapor builds up in the garbage. The moisture absorption increases the ability for swelling and weakening the polymeric bonds. The size and component of compounds that make up the substrate are factors that affect degradation. The second, bacteria, algae, and *actinomycete*, in collaboration with water, affected the structure of fibers and macromolecular adhesives break down. The third, destruction of cementing points and erosion on fiber and resin connections, provides more degradation sites for further attacks of microorganisms. The increase in temperature causes the kinetic energy of the substrate molecules and enzymes to increase, which also contributed for accelerating the degradation process [67]. However, high temperatures cause damage the enzymes called denaturation, while low temperatures can inhibit enzymes working well. The final process of this degradation process is the formation of urea, which can fertilize plants.

Figure 7 shows the relation between the amount of crystalline phase, the distance wavenumber between two optical phonon modes Δ(LO−TO), tensile strength, biodegradation ability for various amount of SPF (1%, 3%, and 5%). By this method, there are two relations: first, the relation between Δ(LO−TO) and crystalline phase and the second, the biodegradation with crystalline phase and tensile strength for various amounts of SPF. Figure 7 shows clearly crystalline phase increase the tensile strength also increase may due to the formation ordered structure as the effect of interfacial complexion between the SPF with starch/chitosan/polypropylene as a matrix [68].

Future work, understand the effects of weather, decomposition of materials under thermal technology, and degradation kinetics. In many cases, the level of soil nutrition, carbon, and nitrogen content are the main factors causing the shift in soil structure and microbial community network. Organic amendments can affect microbial diversity

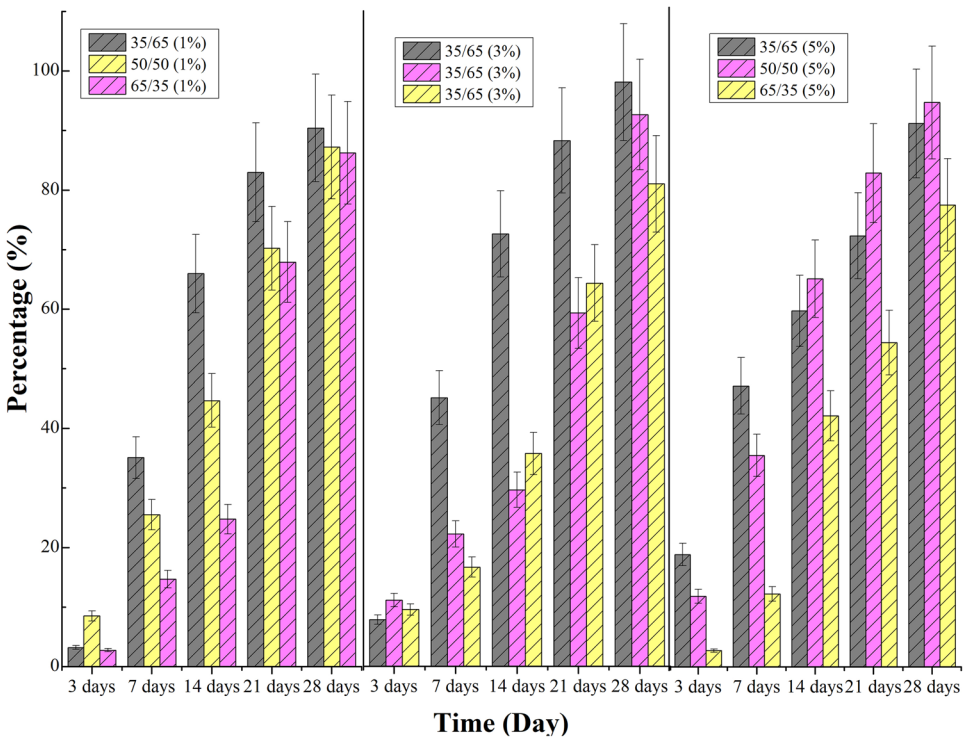

Fig. 5 Biodegradation for bioplastics composite SPF/starch/chitosan/polypropylene with different ratios of starch/chitosan and various amount of SPF in this study

Content courtesy of Springer Nature, terms of use apply. Rights reserved.

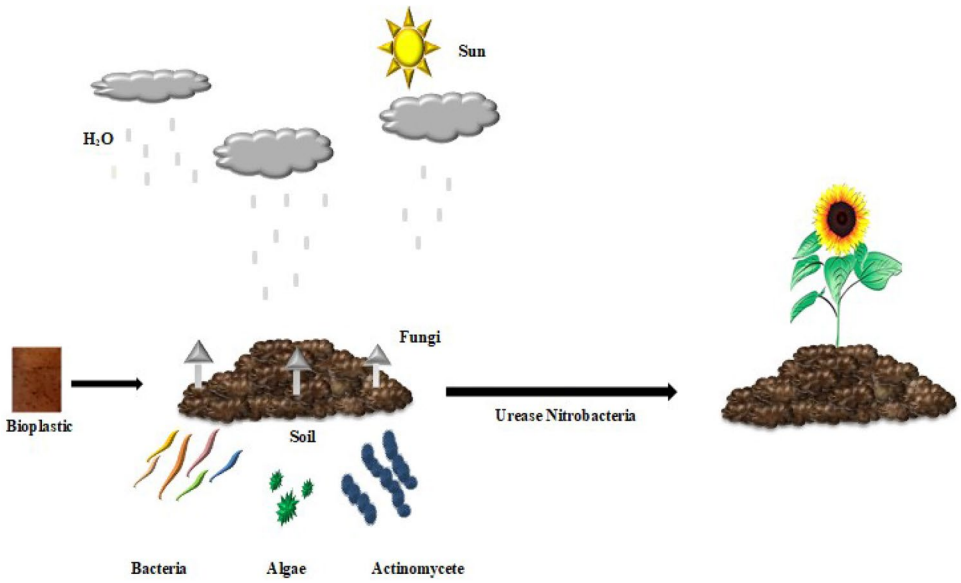

Fig. 6 Illustration of the degradation process of bio-plastic naturally

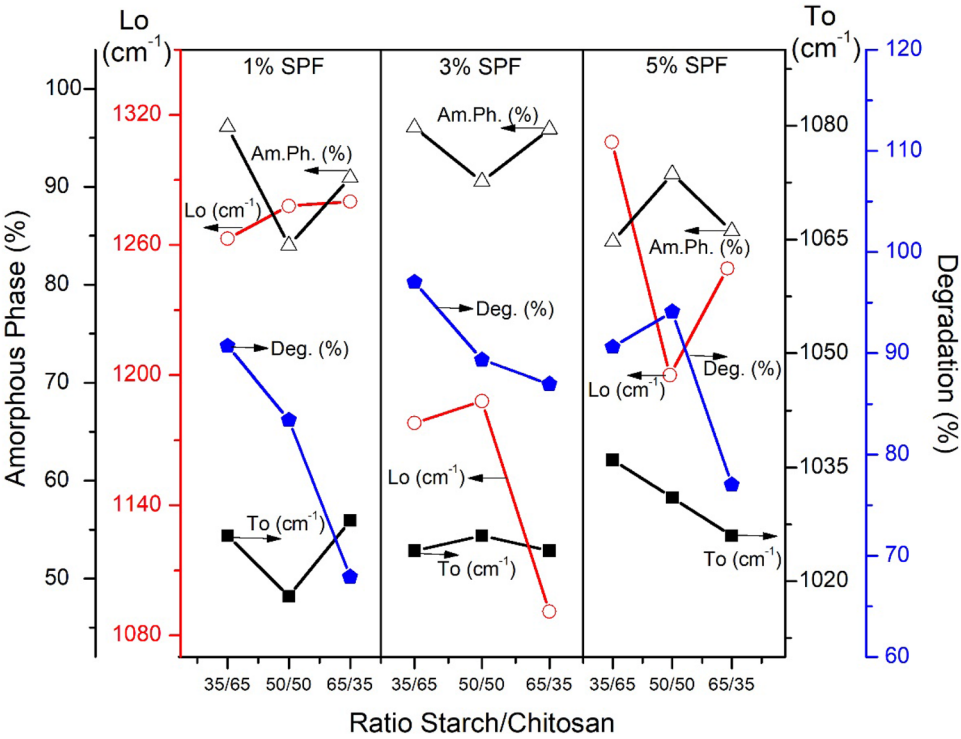

Fig. 7 The relation between structural properties and optical properties with the tensile strength and biodegradation performance

as well as the relative abundance of *copiotrophic* and *oligotrophic* bacteria.

Conclusion

Composite bioplastic SPF/Starch/Chitosan/Polypropylene has been synthesized for the various ratio between starch and chitosan are 35/65, 50/50, and 65/35 with additional SPF for each ratio is 1%, 3%, and 5%. The X-Ray diffraction (XRD) spectra used for determining the amorphous and crystalline phase and Fourier transform infra-red (FTIR) spectroscopy used for determining optical properties. In the form of refractive index (n), extinction coefficient (k), dielectric functions (ε), and energy loss function (Im $(-1/\varepsilon)$) by using Kramers-Kronig (K-K) relations. The crystalline phase is increased with increasing the amount of SPF in composite bioplastic SPF/Starch/Chitosan /Polypropylene for ratio starch/chitosan is 35/65, which consistent with the distance between the wavenumber (Δ) of transversal and

Content courtesy of Springer Nature, terms of use apply. Rights reserved.

longitudinal optical phonon vibration mode. For ratio starch/chitosan is 35/65 shows tensile strength for 1% SPF is 25.02 MPa increase to 63.24 MPa for 3% SPF, similar for 50/50, and 65/35%. The highest tensile strength is 78 MPa for ratio starch/chitosan is 65/35 with 5% SPF indicated that the SPF has better dispersion and interaction in the starch/chitosan/polypropylene matrix. For the effect of SPF on the degradation performance, shows for ratio starch/chitosan 50/50 increase for 1% SPF is 87.23%, for 3% SPF is 92.59%, and for 5% SPF is 94.12%. For composite bioplastic SPF/Starch/Chitosan /Polypropylene in this study, we found that a good correlation between optical properties, structural properties, mechanical properties, and degradation performance for ratio starch/chitosan 35/65 and 50/50 with SPF 1% and 3% in the composite. This study clearly shows, the FTIR spectra could be useful for determining the optical phonon vibration, dielectric function, and energy loss function of composite bioplastic SPF/Starch/Chitosan /Polypropylene. The degradation performance indicated that the bioplastic with additional polypropylene from plastic waste shows a potential solution for decreasing plastic waste in the world.

Acknowledgements This work was supported by the PTM (Penelitian Tesis Magsiter): 1517/UN4.22/PT.01.03/2020 2020 funded by the Indonesian Government (Kemenristek/BRIN).

References

1. Amer ZJA, Saeed AQ (2015) Soil burial degradation of polypropylene/starch blend. Int J Tech Res Appl 3:91–96
2. Estaca JG, Gavara R, Catala R, Munoz PH (2016) The potential of proteins for producing food packaging materials: a review. Packag Technol Sci 29:203–224
3. Samper MD, Bertomeu D, Arrieta MP, Ferri JM, Martines JL (2018) Interference of biodegradable plastics in the polypropylene recycling process. Materials 11:1886
4. Pivawatakarn P, Limmatvapirat C, Sriamorsak P, Anan ML, Nunthanid J, Limmatvapirat S (2015) Effect of glycerol on the properties of tapioca starch film. Adv Mater Res 1060:128–132
5. Wojtasz J, Carlstedt J, Fyhr P, Kocherbitov V (2016) Hydration and swelling of amorphous cross-linked starchmicrospheres. Carbohydr Polym 135:225–233
6. Mitrus M, Moscicki L (2014) Extrusion-cooking of starch protective loose-fillfoams. Chem Eng Res Design 92:778–783
7. Mutmainna I, Tahir D, Gareso PL, Ilyas S, Saludung A (2019) Improving degradation ability of composite starch/chitosan by additional pineapple leaf microfibers for food packaging applications. IOP Conf Series 593:012024
8. Jangong OS, Gareso PL, Mutmainna I, Tahir D (2019) Fabrication and characterization starch/chitosan reinforced polypropylene as biodegradable. IOP Conf Series 1341:082022
9. AL-Oqla FM, Sapuan SM (2014) Natural fiber reinforced polymer composites in industrial applications: feasibility of date palm fibers for sustainable automotive Industry. J Clean Product 66:347–354
10. Atiqah A, Jawaid M, Ishak MR, Sapuan SM (2018) Effect of alkali and silane treatments on mechanical and interfacial bonding strength of sugar palm fibers with thermoplastic polyurethane. J Nat Fibers 15:251–261
11. Lumingkewas RH, Setyadi R, Yanita R, Akbar S, Yuwono AH (2018) Tensile behavior of composite concrete reinforced sugar palm fiber. Eng Mater 777:471–475
12. Atiqah A, Jawaid M, Sapuan SM, Ishak MR, Ausari MNM, Ilyas RA (2019) Physical and thermal properties of treated sugar palm/glass fibre reinforced thermoplastic polyurethane hybrid composites. J Mater Res Technol 8:3726–3732
13. Chaiwong W, Samoh N, Eksomtramage T, Kaewtatip K (2019) Surface-treated oil palm empty fruit bunch fiber improved tensile strength and water resistance of wheat gluten-based bioplastic. Compos Part B 176:107331
14. Syafri E, Jamaluddin WS, Irwan A, Asrofi M, Sari NH, Fudholi A (2019) Characterization and properties of cellulose microfibers from water hyacinth filled sago starch biocomposites. Int J Biol Macromol 137:119–125
15. Aguilar NM, Arteaga-Cardona F, de Anda Reyes ME, Gervacio-Arciniega JJ, Salazar-Kuri U (2019) Magnetic bioplastics based on isolated cellulose from cotton and sugarcane bagasse. Mater Chem Phys 238:121921
16. Aguilar JM, Bengoechea C, Pérez E, Guerrero A (2020) Effect of different polyols as plasticizers in soy based bioplastics. Indus Crops Products 153:112522
17. Emadian SM, Onay TT, Demirel B (2017) Biodegradation of bioplastics in natural environments. Waste Manage 59:526–536
18. Perotto G, Simonutti R, Ceseracciu L, Mauri M, Besghini D, Athanassiou A (2020) Water-induced plasticization in vegetable-based bioplastic films: A structural and thermo-mechanical study. Polymer 200:122598
19. Alashwal BY, Bala MS, Gupta A, Sharma S, Mishra P (2019) Water-induced plasticization in vegetable-based bioplastic films: a structural and thermo-mechanical study. J King Saud Uni Sci 32:853–857
20. Heredia-Guerrero JA, Goldoni L, Benıtez JJ, Davis A, Ceseracciu L, Cingolani R, Bayer IS, Heinze T, Koschella A (2017) Cellulose-polyhydroxylated fatty acid ester-based bioplastics with tuning properties: acylation via a mixed anhydride system. Carbohydr Polymers 173:312–320
21. Tsang YF, Kumar V, Samadar P, Yang Y, Lee J, Ok YS, Song H, Kim KH, Kwon EE, Jeon YJ (2019) Production of bioplastic through food waste valorization. Environ Int 127:625–644
22. Karua CS, Sahoo A (2020) Production of bioplastic through food waste valorization. Materials Today: Proceedings In Press.
23. Atiqah A, Maleque MA, Jawaid M, Iqbal M (2014).\ Production of bioplastic through food waste valorization. Composites: Part B, 56:68–73.
24. Han Q, Zhao L, Lin P, Zhu Z, Nie K, Yang F, Wang L (2020) Poly(butylene succinate) biocomposite modified by amino functionalized ramie fiber fabric towards exceptional mechanical performance and biodegradability. React Funct Polymers 146:104443
25. Dash C, Das A, Bisoyi DK (2020) Influence of pretreatment on mechanical and dielectric properties of short sunn hemp fiber-reinforced polymer composite in correlation with fine structure of the fiber. Journal of Composite Materials 0(0):1–15.
26. Khorrami GhH, Zak AK, Kompany A, yousefi R, (2012) Optical and structural properties of X-doped (X = Mn, Mg, and Zn) PZT nanoparticles by Kramers-Kronig and size strain plot methods. Ceramics International 38:5683–5690
27. Zak AK, Ghanbari A, ShekoftehNarm T (2017) The effect of molybdenum on optical properties of ZnO nanoparticles in Ultraviolet-Visible region. Adv Powder Technol 28(11):2980–2986
28. Zak AK, Abd. Majid WH, (2011) Effect of solvent on structure and optical properties of PZT nanoparticles prepared by sol-gel method, in infrared region. Ceram Int 37:753–758

Content courtesy of Springer Nature, terms of use apply. Rights reserved.

29. Asrofi M, Abral H, Kasim A, Pratoto A, Mahardika M, Hafizulhaq F (2018) Mechanical properties of a water hyacinth nanofiber cellulose reinforced thermoplastic strach bionanocomposite: effect of ultrasonic vibration during processing. Fibers 6(2):40
30. Bourtoom T, Chinnan MS (2008) Preparation and properties of rice starche-chitosan blend biodegradable film. LWT - Food Sci Technol 41:1633–1641
31. Ilyas RA, Sapuan SM, Ibrahim R, Abral H, Ishak MR, Zainudin ES, Asrofi M, Atikah MSN, Huzaifah MRM, Radzi AM, Azammi AMN, Shararuzaman MA, Nurazzi NM, Syafri E, Sari NH, Norrahmi MNF, Jumaidin R (2019) Sugar palm (Arenga pinnata (Wurmb) Merr) cellulosic fibre hierarchy: a comprehensive approach from macro to nano scale. J Mater Res Technol 8(3):2753–2766
32. Tahir D, Ilyas S, Abdullah B, Armynah B, Kim K, Kang HJ (2019) Modification in electronic, structural, and magnetic properties based on composition of composites Copper (II) Oxide (CuO) and Carbonaceous material. Mater Res Express 6:035705
33. Ilyas S, Heryanto AB, Tahir D (2019) X-ray diffraction analysis of nanocomposite Fe_3O_4/activated carbon by Williamson-Hall and size-strain plot methods. Nano-Struct Nano-Objects 20:100396
34. Heryanto H, Abdullah B, Tahir D (2018) Analysis of structural properties of X-ray diffraction for composite copper-activated carbon by modified Williamson-Hall and size-strain plotting methods. J Phys: Conf Series 1080:012007
35. Abdullah B, Ilyas S, Tahir D (2018) Nanocomposites Fe/Activated Carbon/PVA for MicrowaveAbsorber: Synthesis and Characterization. Journal of Nanomaterials 2018:ID 982326.
36. Izwana SM, Sapuan SM, Zuhria MYM, Mohamed AR (2020) effects of benzoyl treatment on NaOH treated sugar palm fiber: tensile, thermal, and morphological properties. J Mater Res Technol 9(3):5805–5814
37. Harkins AL, Duri S, Kloth LC, Tran CD (2014) Chitosan–cellulose composite for wound dressing material. Part 2. Antimicrobial activity, blood absorption ability, and biocompatibility. Biomed Mater Res Part B 102B:1199–1206
38. Perotti GF, Kijchavengkul T, Auras RA, Constantino VRL (2017) Nanocomposites based on cassava strach and chitosan modified clay: physico – mechanical properties and biodegradability in simulated compost soil. J Braz Chem Soc 24(4):649–658
39. Yu Z, Li B, Chu J, Zhang P (2018) Silica in situ enhanced PVA/chitosan biodegradable films for food packages. Carbohydr Polymers 184:214–220
40. Obasi HC, Igwe IO, Madufor IC (2013) Effect of Soil Burial on Tensile Properties of Polypropylene/Plasticized Cassava Starch Blends. Materials Science and Engineering 2013:ID 326538.
41. Kubovský I, Kačíková D, Kačík F (2020) Structural changes of oak wood main components caused by thermal modification. Polymers 12(2):485
42. El-Hendawy AA (2006) Variation in the FTIR spectra of a biomass under impregnation, carbonization and oxidation conditions. J. Anal Appl Pyrolysis 75:159–166
43. Suryani S, Heryanto H, Rusdaeni R, Fahri AN, Tahir D (2020) Quantitative analysis of diffraction and infra-red spectra of composite cement/$BaSO_4$/Fe3O4 for determining correlation between attenuation coefficient, structural and optical properties. Ceram Int 46:18601–18607
44. Kangarlou H, Aghgonbad MM, Abdollahi A (2015) Investigation about the effect of annealing temperatures in the presenceof oxygen flow on optical and electronic properties of titanium nanolayers by using Kramers-Kronig and DFT methods. Mater Scie Semiconductor Process 30:1–8
45. Norouzzadeh P, Mabhouti Kh, Golzan MM, Naderali R (2020) Investigation of structural, morphological and optical characteristics of Mn subsitituted Al-doped ZnO NPs: A urbach energy and Kramers-Kronig study. Optik 204:64227
46. Tan GL, DeNoyer LK, French RH, Guittet MJ, Gautier-Soyer M (2005) Kramers-Kronig transform for the surface energy loss function. J Electron Spectrosc Related Phenomena 142:97–103
47. Tahir D, Tougaard S (2012) Electronic and optical properties of Cu, CuO and Cu_2O studied by electron spectroscopy. J. Phys.: Condens. Matter 24:175002.
48. Shin HC, Tahir D, Seo S, Denny YR, Oh SK, Kang HJ, Heo S, Chung JG, Lee JC, Tougaard S (2012) Reflection electron energy loss spectroscopy for ultrathin gate oxide materials. Surf Interface Anal 44:623–627
49. Tahir D, Tougaard S (2012) Electronic and optical properties of selected polymers studied by reflection energy loss spectroscopy. J Appl Phys 111:054101
50. Tahir D, Kraaer J, Tougaard S (2014) Electronic and optical properties of Fe, Pd, Ti studied by reflection electron energy loss spectroscopy. J Appl Phys 115:243508
51. Tahir D, Ilyas SDA, Kang HJ (2011) Band aligment of ultrathin Gizo/SiO_2/Si heterostructure determined by electron spectroscopy. Makara Sains 15:193–196
52. Tahir D, Ilyas S, Abdullah B, Armynah B, Kang HJ (2018) Electronic properties of composite Iron (II, III) Oxide (F_e3_O4) carbonaceous absorber materials by electron spectroscopy. J Electron Spectrosc Related Phenomena 229:47–51
53. Tahir D, Oh SK, Kang HJ, Tougaard S (2016) Quantitative analysis of reflection electron energy loss spectra to determine electronic and optical properties of Fe-Ni alloy thin films. J Electron Spectrosc Related Phenomena 206:6–11
54. Denny YR, Shin HC, Seo S, Oh SK, Kang HJ, Tahir D, Heo S, Chung JG, Lee JC, Tougaard S (2012) Electronic and optical properties of hafnium indium zinc oxide thin film by XPS and REELS. J Electron Spectrosc Related Phenomena 185:18–22
55. Suryani S, Heryanto Tahir D (2020) Stopping powers and inelastic mean free path from quantitative analysis of experimental REELS spectra for electrons in Ti, Fe, Ni, and Pd. Surf Interface Anal 52(1–2):16–22
56. Tahir D, Oh SK, Kang HJ, Tougaard S (2016) Composition dependence of dielectric and optical properties of Hf-Zr-silicate thin films grown on Si(100) by atomic layer deposition. Thin Solid Films 616:425–430
57. Ghasemifard M, Hosseini SM, Khorrami GhH (2009) Synthesis and structure of PMN-PT ceramic nanopowder free from pyrochlore phase. Ceram Int 35:2899–2905
58. Legan L, Leskovar T, Cresnar M, Cavalli F, Innocenti D, Ropret P (2020) Non-invasive reflection FTIR characterization of archaeological burnt bones: Reference database and case studies. J Cult Heritage 41:13–26
59. Tahir D, Suarga, Sari NH, Yulianti, (2015) Stopping powers and in elastic mean free path of 200eV–50 keV electrons in polymer PMMA, PE, and PVC. Appl Radiation Isotopes 95:59–62
60. Nurhasmi, Heryanto, Fahri AN, Ilyas S, Ansar A, Abdullah B, Tahir D (2020) Study on Optical Phonon Vibration and Gamma Ray Shielding Properties of Composite Geopolymer Fly Ash-Metal. Radiat Phys Chem (In Press)
61. Lahsmin YK, Heryanto H, Ilyas S, Fahri AN, Abdullah B, Tahir D (2020) Optical properties determined from infrared spectroscopy and structural properties from diffraction spectroscopy of composites Fe/CNs/PVA for electromagnetic wave absorption. Opt Mater (In Press).
62. Ibrahim MIJ, Sapuan SM, Zainudin ES, Zuhri MYM (2020) Preparation and characterization of cornhusk/sugar palm fiber reinforced Cornstrach-based hybrid composites. J Mater Res Technol 9(1):200–211
63. Navarro YM, Soukup K, Jandová V, Gómez MM, Solis JL, Cruz JF, Siche R, Šolcová O, Cruz GJF (2019) Strach/chitosan/glycerol film produced from low-value biomass: effect of starch source and wight ratio on film properties. J Phys: Conf. Series 1173:012008

Content courtesy of Springer Nature, terms of use apply. Rights reserved.

64. Mierzwa-Hersztek M, Gondek K, Kopeć M (2019) Degradation of polyethylene and biocomponent-derived polymer materials: an overview. J Polym Environ 27:600–611
65. Lubis M, Harahap MB, Ginting MHS, Sartika M, Azmi H (2016) Effect of microcrystalline cellulose (MCC) from sugar palm fibres and glycerol additionon mechanical properties of bioplastic from avocado seed strach (Parsea Americana Mill). ECBA 31:1–10
66. Sumaiyah, Wirijosentono B, Karsono, Nasution MP, Gea S (2014) Preparation and characterization of nanocrystalline cellulose from sugar palm bunch (Arenga pinnata (Wurmb) Merr.). Int. J. PharmTech Res. 6(2):814–820
67. Sun E, Liao G, Zhang Q, Qu P, Wu G, Huang H (2019) Biodegradable copolymer-based composites made from straw fiber for biocomposite flowerpots application. Composites Part B 165:193–198
68. Mukhtar I, Leman Z, Ishak MR, Zainudin ES (2016) Sugar palm fiber and its composites: a review of recent developments. BioResources 11(4):10756–10782

Publisher's Note Springer Nature remains neutral with regard to jurisdictional claims in published maps and institutional affiliations.

Content courtesy of Springer Nature, terms of use apply. Rights reserved.

Terms and Conditions

Springer Nature journal content, brought to you courtesy of Springer Nature Customer Service Center GmbH (“Springer Nature”).
Springer Nature supports a reasonable amount of sharing of research papers by authors, subscribers and authorised users (“Users”), for small-scale personal, non-commercial use provided that all copyright, trade and service marks and other proprietary notices are maintained. By accessing, sharing, receiving or otherwise using the Springer Nature journal content you agree to these terms of use (“Terms”). For these purposes, Springer Nature considers academic use (by researchers and students) to be non-commercial.
These Terms are supplementary and will apply in addition to any applicable website terms and conditions, a relevant site licence or a personal subscription. These Terms will prevail over any conflict or ambiguity with regards to the relevant terms, a site licence or a personal subscription (to the extent of the conflict or ambiguity only). For Creative Commons-licensed articles, the terms of the Creative Commons license used will apply.
We collect and use personal data to provide access to the Springer Nature journal content. We may also use these personal data internally within ResearchGate and Springer Nature and as agreed share it, in an anonymised way, for purposes of tracking, analysis and reporting. We will not otherwise disclose your personal data outside the ResearchGate or the Springer Nature group of companies unless we have your permission as detailed in the Privacy Policy.
While Users may use the Springer Nature journal content for small scale, personal non-commercial use, it is important to note that Users may not:

1. use such content for the purpose of providing other users with access on a regular or large scale basis or as a means to circumvent access control;
2. use such content where to do so would be considered a criminal or statutory offence in any jurisdiction, or gives rise to civil liability, or is otherwise unlawful;
3. falsely or misleadingly imply or suggest endorsement, approval , sponsorship, or association unless explicitly agreed to by Springer Nature in writing;
4. use bots or other automated methods to access the content or redirect messages
5. override any security feature or exclusionary protocol; or
6. share the content in order to create substitute for Springer Nature products or services or a systematic database of Springer Nature journal content.

In line with the restriction against commercial use, Springer Nature does not permit the creation of a product or service that creates revenue, royalties, rent or income from our content or its inclusion as part of a paid for service or for other commercial gain. Springer Nature journal content cannot be used for inter-library loans and librarians may not upload Springer Nature journal content on a large scale into their, or any other, institutional repository.
These terms of use are reviewed regularly and may be amended at any time. Springer Nature is not obligated to publish any information or content on this website and may remove it or features or functionality at our sole discretion, at any time with or without notice. Springer Nature may revoke this licence to you at any time and remove access to any copies of the Springer Nature journal content which have been saved.
To the fullest extent permitted by law, Springer Nature makes no warranties, representations or guarantees to Users, either express or implied with respect to the Springer nature journal content and all parties disclaim and waive any implied warranties or warranties imposed by law, including merchantability or fitness for any particular purpose.
Please note that these rights do not automatically extend to content, data or other material published by Springer Nature that may be licensed from third parties.
If you would like to use or distribute our Springer Nature journal content to a wider audience or on a regular basis or in any other manner not expressly permitted by these Terms, please contact Springer Nature at

onlineservice@springernature.com